2019 16th International Conference on Electrical Engineering, Computing Science and Automatic Control (CCE) Mexico City, Mexico. September 11-13, 2019

Nonsingular Fast Terminal Sliding Mode Control for an Autonomous Underwater Vehicle

Angel E. Zamora Suarez
LAFMIA-UMI 3175
CINVESTAV-IPN
Mexico city, Mexico
email: angel_esfm2001@hotmail.com

Miguel Angel Garcia Rangel
LAFMIA-UMI 3175
CINVESTAV-IPN
Mexico city, Mexico
email: miguelgarciar@cinvestav.mx

Adrian Manzanilla Magallanes
LAFMIA-UMI 3175
CINVESTAV-IPN
Mexico city, Mexico
email: amanzanilla@cinvestav.mx

Rogelio Lozano Leal
Sorbonne Universités - Heudiasyc UMR 7253
Université de Technologie de Compiegne
Compiegne, France
email: rlozano@hds.utc.fr

Sergio Salazar Cruz
LAFMIA-UMI 3175
CINVESTAV-IPN
Mexico city, Mexico
email: sergio.salazar.cruz@gmail.com

Filiberto Muñoz Palacios
LAFMIA-UMI, CINVESTAV
Cátedras CONACYT
Mexico city, Mexico
email: filiberto.munoz@cinvestav.mx

***Abstract*—In this article, the mathematical model based on quaternions for an underwater autonomous vehicle (AUV) of 6 DOF is developed, to avoid singularities that appear in the representation of Euler's angles. For this vehicle, a Non-Singular Fast Terminal Sliding Mode Control (NFTSMC) non-linear controller is proposed, which presents a variation in the sliding surface that guarantees a high rate of convergence of the states in finite time. To verify the stability of the closed-loop control system, an approach of the Lyapunov theory is used, ensuring the convergence in finite time of the tracking errors to a bounded region in the presence of model uncertainties and disturbances. Simulations results are presented to illustrate the efficiency of the developed strategy.**

***Index Terms*—AUV, NFTSMC, quaternions, underwater vehicle, trajectory tracking**

I. Introduction

Nowadays, Unmanned Underwater Vehicles (UUV's) have positioned themselves as important tools for the industry, as well as for the researchers, since they have allowed performing various tasks that include the exploration of the marine mantle, inspection of structures, oceanographic surveys, acquisition of physical variables, taking biological samples, etc, [1].

UUV's are classified by their operation: remotely operated vehicles (ROV's) and autonomous underwater vehicles (AUV's). ROV's are usually operated remotely by a cable to a station and controlled by an operator. Moreover, AUV's refer to robots that perform particular tasks without human intervention. However, there are different challenges in these vehicles due to their non-linear dynamics and uncertainties in the model. Not to mention the external disturbances generated by the water currents and the movement of the waves [2].

In order to perform a task in a marine vehicle a certain level of autonomy is required. Due to this, the analysis of the dynamics of the vehicle and the management of its behavior is important. In the literature, manuscripts focused on the analysis of the dynamic model of an underwater vehicle have been proposed; in [3], [4] and [5] different mathematical representations are proposed to study the behavior of these vehicles considering different parameters, such as the aggregate mass, the hydrodynamic drag force and the restorative forces. In this work, we focus on the representation by quaternions proposed in [6] by means of which we avoid the singularities existing in the representation of Euler angles.

Some authors have used the representation of quaternions to globally stabilize different types of platforms, in [7] they propose a scheme of control of quaternion to stabilize an unmanned aerial vehicle. Whereas, in [8] a motion simulation platform for a submarine vehicle is presented including an autopilot system through the use of quaternions that determine the stability of the turn and the capacity of the course change during the test. Moreover, in [9] the control of a UUV of 6 DOF is discussed, the representation of unitary quaternions is used to manage the attitude control and because it is free of singularity.

As a mean to control this type of vehicle several robust control strategies have been proposed, in [10] a three-axis attitude tracking control of an AUV based on a sliding mode control (SMC) approach and an observer of extended state of finite time guarantee the tracking trajectory of the system to closed loop with convergence of finite time, even with the existence of disturbances and non-linearities. An adaptive tracking control using neural networks and a reinforcement algorithm capable of handling parametric uncertainties and perturbations for a fully actuated AUV is shown in [11]. Furthermore, in [12] a robust, non-linear hierarchical controller is designed for trajectory tracking subject to uncertainties by backstepping and sliding mode techniques where they achieve asymptotic stability even when various random uncertainties are introduced. In [13] a depth controller using a NFTSMC is

978-1-7281-4840-3/19/$31.00 ©2019 IEEE

developed for an underwater vehicle.

The main contribution of this work is a dynamic representation of an underwater vehicle of 6DOF through the use of quaternions, as well as the development of a MIMO NFTSMC that guarantees tracking errors converge to a bounded region in finite time. Moreover, the control strategy developed presents robustness in presence of unmodeled dynamics and unknown disturbances.

The outline of the document is described as follows: mathematical preliminaries are presented in the Section II, the dynamic model of the vehicle is described in Section III, the control strategy using sliding mode technique is shown in Section IV. Finally, the results of the trajectory tracking simulation tests for a fully autonomous operation can be seen in the Section V, conclusions and future developments about this work are detailed in the Section VI.

II. Mathematical preliminaries

The quaternion q is defined as

$$q = q_0 + q_x i + q_y j + q_z k = q_0 + \mathfrak{q}; \tag{1}$$

where $i^2 = j^2 = z^2 = ijk = 1$, $\mathfrak{q}$ is the imaginary part and q_0 is the real part. The product between two quaternions p and q is defined as

$$p \quad q = p_0 q_0 \quad \mathfrak{p} \quad \mathfrak{q} + p_0 \mathfrak{q} + q_0 \mathfrak{p} + \mathfrak{p} \quad \mathfrak{q}; \tag{2}$$

with $\mathfrak{p}$ $\mathfrak{q}$ and $\mathfrak{p}$ $\mathfrak{q}$ being the dot product and the cross product, respectively. The inverse of a quaternion is

$$q^{-1} = \frac{q}{kqk}; \tag{3}$$

where $q = q_0 \quad \mathfrak{q}$ and $kqk = \sqrt{q_0^2 + q_x^2 + q_y^2 + q_z^2}$. If $kqk = 1$, then, it is defined as a unitary quaternion. For unitary quaternions, their natural logarithmic is defined as

$$\frac{\tilde{}}{2} = \ln(q) = \begin{cases} \frac{\mathfrak{q}}{k\mathfrak{q}k} \arccos q_0 & \text{if } k\mathfrak{q}k \neq 0 \\ 0 & \text{if } k\mathfrak{q}k = 0; \end{cases} \tag{4}$$

where $\tilde{}$ is the axis-angle representation, and $\dot{} = \tilde{}$ is the vehicle's angular velocity. For more details see [14] and [15].

III. Mathematical model of the underwater vehicle

The representation using quaternions of the dynamic model for an underwater vehicle considers two coordinate frames, a body reference frame O_B and an inertial frame O_I, see Figure 1. The equations that represent this system are given by the

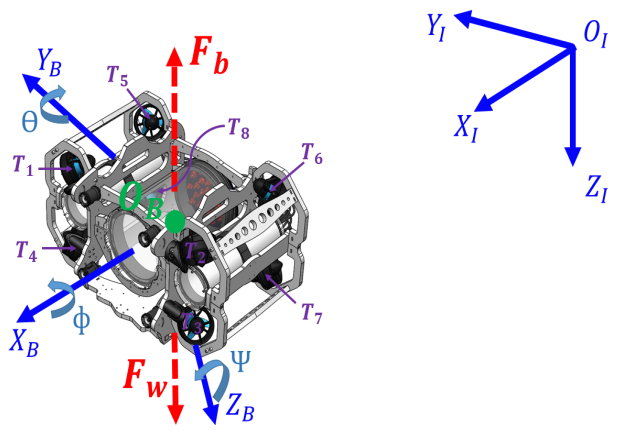

Fig. 1. The references of the coordinate frames for the submarine vehicle are, a fixed frame of body O_B moves with respect to a fixed frame of inertia to the earth O_I. Moreover, the location of the thrusters T_i in the structure robot is shown.

model proposed by Fossen in [3], [16] and can be expressed as

$$\begin{aligned} M\dot{} + C(\ ) \quad + D(\ ) \quad + g(q) = \quad + \\ \dot{q} = \frac{1}{2} q \quad \dot{} \\ \dot{P}_I = q \quad \forall \quad q \ ; \end{aligned} \tag{5}$$

where $M \ 2 \ \mathbb{R}^{6 \ 6}$ represents the inertia matrix, $C(\ ) \ 2 \ \mathbb{R}^{6 \ 6}$ define the Coriolis matrix, $D(\ ) \ 2 \ \mathbb{R}^{6 \ 6}$ is the damping matrix, $g(q) \ 2 \ \mathbb{R}^{6 \ 1}$ represents the vector of gravitational and buoyancy forces, $= [X; Y; Z; K; M; N]^T \ 2 \ \mathbb{R}^{6 \ 1}$ is the vector of control inputs and denotes the vector of disturbances. P_I is the position of the vehicle in the inertial system, q is the rotation quaternion of the vehicle and $= [\nu^T; \dot{}^T]^T$ defines the linear and angular velocity vector seen in the body system, respectively, with $\nu^T = [u; v; w]^T$ and $\dot{}^T = [p; q; r]^T$. Fossen's model with Euler's angles is very similar to that of quaternions, which is defined as

$$\begin{aligned} M\dot{} + C(\ ) \quad + D(\ ) \quad + g(\ ) = \quad + \\ \dot{} = J(\ ) \end{aligned} \tag{6}$$

where $= [P_I^T; \tilde{}^T]^T$ and $\tilde{} = [\ ; \ ; \ ]^T$ are the Euler angles describing the orientation of the vehicles body fixed frame with respect to the earth-fixed frame (roll, pitch, and yaw).

The vector is denoted by the following equation

$$= \begin{bmatrix} \frac{1}{2} \sum_{i=0}^{1} \sum_{j=1}^{4} (\ 1)^i F_{4i+j} \\ \frac{1}{\sqrt{2}} \sum_{i=0}^{7} (\ 1)^i F_{i+1} \\ \frac{1}{2} \sum_{i=0}^{3} \sum_{j=1}^{2} (\ 1)^i F_{2i+j} \\ \frac{l_y + \sqrt{2} l_z}{2} \sum_{i=0}^{1} \sum_{j=1}^{4} (\ 1)^{i+j+1} F_{2j+i-1} \\ \frac{l_x + l_z}{2} \sum_{i=0}^{1} \sum_{j=0}^{1} \sum_{k=1}^{2} (\ 1)^{2k+j+i} F_{4i+2j+k} \\ \frac{l_y - \sqrt{2} l_x}{2} \sum_{i=0}^{1} \sum_{j=1}^{4} (\ 1)^{i+j+1} F_{4i+j} : \end{bmatrix} \tag{7}$$

The forces and moments that act in the vehicle are represented in Figure 2, where it can be seen that the thrusters have a

rotation of $\frac{}{4}$ in two of their axes, with a distance $l_x; l_y$ and l_z, with respect to the center of gravity C_G. Assuming that the

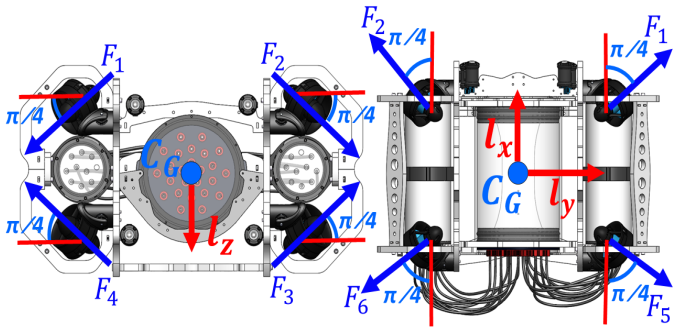

Fig. 2. The forces acting on the submarine are due to 8 thrusters. The propellers are bidirectional, so the combination of forces is used to generate the movement of rotation and translation. Propellers 1, 3, 6 and 8 use propellers in a clockwise direction, whilst 2, 4, 5 and 7 are counterclockwise, canceling the reactive moments.

matrix M, $C(\ )$ and the vector $g(q)$ of the equation (7) are known, and they can be defined as follows: $M = \text{diag}(m - X_{\dot{u}};\ m - Y_{\dot{v}};\ m - Z_{\dot{w}};\ I_{xx} - K_{\dot{p}};\ I_{yy} - M_{\dot{q}};\ I_{zz} - N_{\dot{r}})$, where m is the vehicle mass. I_{xx}, I_{yy} and I_{zz} are the elements of the inertia matrix. $X_{\dot{u}}$, $Y_{\dot{v}}$, $Z_{\dot{w}}$, $K_{\dot{p}}$, $M_{\dot{q}}$ and $N_{\dot{r}}$ are the elements of the aggregate mass. Because the vehicle travels at low speeds, less than $2m/s$, and the symmetry of the vehicle shape, the C matrix can be defined as

$$C = C_A + C_{RB}; \tag{8}$$

where the matrix C_{RB} denotes the Coriolis matrix of the rigid body and has the following structure

$$C_{RB} = \begin{bmatrix} 0 & 0 & 0 & 0 & C_{R15} & C_{R16} \\ 0 & 0 & 0 & C_{R24} & 0 & C_{R26} \\ 0 & 0 & 0 & C_{R34} & C_{R35} & 0 \\ 0 & C_{R42} & C_{R43} & 0 & C_{R45} & C_{R46} \\ C_{R51} & 0 & C_{R53} & C_{R54} & 0 & C_{R56} \\ C_{R61} & C_{R62} & 0 & C_{R64} & C_{R65} & 0 \end{bmatrix}; \tag{9}$$

with $C_{R15} = C_{R51} = C_{R42} = C_{R24} = mw$; $C_{R61} = C_{R43} = C_{R34} = C_{R16} = vm$; $C_{R62} = C_{R53} = C_{R35} = C_{R26} = um$; $C_{R54} = C_{R45} = I_{zz}r$; $C_{R64} = C_{R46} = I_{yy}q$ and $C_{R65} = C_{R56} = I_{xx}p$. The Coriolis matrix of aggregate mass C_A is given by

$$C_A = \begin{bmatrix} 0 & 0 & 0 & 0 & C_{A15} & C_{A16} \\ 0 & 0 & 0 & C_{A24} & 0 & C_{A26} \\ 0 & 0 & 0 & C_{A34} & C_{A35} & 0 \\ 0 & C_{A42} & C_{A43} & 0 & C_{A45} & C_{A46} \\ C_{A51} & 0 & C_{A53} & C_{A54} & 0 & C_{A56} \\ C_{A61} & C_{A62} & 0 & C_{A64} & C_{A65} & 0 \end{bmatrix}; \tag{10}$$

where $C_{A51} = C_{R15} = C_{R42} = C_{R24} = Z_{\dot{w}}w$; $C_{R61} = C_{R43} = C_{R34} = C_{R16} = Y_{\dot{v}}v$; $C_{R62} = C_{R53} = C_{R35} = C_{R26} = X_{\dot{u}}u$; $C_{R54} = C_{R45} = N_{\dot{r}}r$; $C_{R64} = C_{R46} = M_{\dot{q}}q$ and $C_{R65} = C_{R56} = K_{\dot{p}}p$. Finally, the gravity vector is denoted by the following equation

$$g(q) = \begin{matrix} q \\ \not{r}_b \end{matrix} \begin{matrix} [B \quad W] \\ q \quad W \end{matrix} \begin{matrix} q \\ q \end{matrix}; \tag{11}$$

where W is the weight, B is the buoyancy force. In this work, we assume that the coefficients of the hydrodynamic damping matrix are unknown. However, to conduct a more realistic simulation, the equation that defines the damping matrix is given by $D(\ ) = diag(X_u \quad X_{u_c}|u|; \quad Y_v \quad Y_{v_c}|v|; \quad Z_w \quad Z_{w_c}|w|; \quad K_p \quad K_{p_c}|p|; \quad M_q \quad M_{q_c}|q|; \quad N_r \quad N_{r_c}|r|)$, where $X_u; Y_v; Z_w; K_p; M_q; N_r$ are the linear coefficients of damping and $X_{u_c}; Y_{v_c}; Z_{w_c}; K_{p_c}; M_{q_c}; N_{r_c}$ are the quadratic damping parameters.

IV. Controller Design

In this section, the development of the NFTSMC strategy is presented. The NFTSMC is used to control the dynamic model (5) represented in quaternions. In order to highlight the advantages of the NFTSMC strategy, a FTSM controller is presented and applied to the dynamic model (6) represented in Euler's angles.

A. NFTSM Controller

Consider that $M, C(\ )$ and $g(q)$ are known, then the following control law for the equation (5) is proposed

$$= C(\ ) \quad + g(q) + M \begin{matrix} " \\ q \\ \not{r}_d + \end{matrix} \begin{matrix} h \\ \dot{P}_{I_d} + \ _{v_2} \\ \ _{!_2} \end{matrix} \begin{matrix} i \\ q + \not{r} \quad w \end{matrix} \begin{matrix} # \\ ; \end{matrix} \tag{12}$$

where $\not{r}_d$ and P_{I_d} are the angular velocity desired and the position desired in the inertial frame, respectively. $_{v_2}$ and $_{!_2}$ are new virtual control inputs to be designed latter. Substituting (12) in (5) we obtain

$$\begin{matrix} \dot{P}_I \quad \dot{P}_{I_d} = \tilde{} _{v_2} + \ _{v_2} \\ \not{r}_I \quad \not{r}_d = \tilde{} _{!_2} + \ _{!_2}; \end{matrix} \tag{13}$$

with $_2 = [(q \quad \tilde{} _{v_2} \quad q\ )^T; \tilde{} ^T_{!_2}]^T$ where $[\tilde{} ^T_{v_2}; \tilde{} ^T_{!_2}]^T = M^{-1}(\quad D\ )$. Define $e = [P_I^T \quad P_d^T; 2\ln(q_d \quad q)^T]^T$ (if the real part of $R(q_d \quad q) < 0$ with $R(q) = q_0$, then we define the error as $e = [P_I^T \quad P_d^T; 2\ln(\ q_d \quad q)^T]^T$) and $_2 = [\ ^T_{v_2}; \ ^T_{!_2}]^T$. Based in [13] the following sliding surface $s \in \mathbb{R}^6$ is proposed

$$s = e + A\text{sig}(e)^{\quad} + B\text{sig}(\underline{e}) \tag{14}$$

$$\underline{s} = |e| \quad ^{I_6} \ ^6[K_1 s + K_2 \text{sig}(s)^{M_n}]; \tag{15}$$

where $K_1 = \text{diag}(k_{1:1}; \dots; k_{1:6})$, $K_2 = \text{diag}(k_{2:1}; \dots; k_{2:6})$, $A = \text{diag}(A_1; \dots; A_6)$, $B = \text{diag}(B_1; \dots; B_6)$, $= \text{diag}(\ _1; \dots; \ _6)$, $= \text{diag}(\ _1; \dots; \ _6)$, $M_n = \text{diag}(M_1; \dots; M_6)$. With $k_{1:i}$, $k_{2:i}$, A_i, B_i, M_i as positive constants and $1 < \ _i < 2$, $\ _i > \ _i$ for $i = 1; \dots; 6$. The function sig is defined as

$\text{sig}(\ )^{\%} \triangleq [j\ _1 j^{\%_1}\text{sign}(\ _1); :::; j\ _6 j^{\%_6}\text{sign}(\ _6)]^T$, $\% = \text{diag}(\%_1; :::; \%_6)$ and the function of the absolute value of the vector by $jej\ ^{I_{6\ 6}} = \text{diag}\ je_1 j^{\ 1\ 1}; :::; je_6 j^{\ 6\ 1}$.

Theorem 1

For the dynamic model of an AUV (5), if the sliding surface is chosen as (14), the reaching law is chosen as (15) and the continuous NFTSMC is designed as

$$\begin{aligned} _2 = \quad & {}^1B\ ^1[K_1 s + K_2 \text{sig}(s)^{M_n} + \text{sig}(\dot{e})^{2I_{6\ 6}} \quad + \\ & A\ jej\ ^{I_{6\ 6}}\text{sig}(\dot{e})^{2I_{6\ 6}}\ ]; \end{aligned} \tag{16}$$

where $\dot{}_d$ and P_{I_d} are the angular velocity desired and the position desired in the inertial frame, respectively. Then the system trajectory will converge to the neighborhood of sliding surface $s = 0$ as

$$\begin{aligned} ksk_1 \quad _3 &= \min f\ _{3:1};\ _{3:2}g \\ _{3:1} &= k\ \ ^1B\ ^1K_1 H(\ _2)\ ^1k_1 \\ _{3:2} &= ksig(\ \ ^1B\ ^1K_2 H(\ _2)\ ^1)^{M_n} k_1 \end{aligned} \tag{17}$$

in finite time, where $H(p) = \text{diag}(p_1; :::; p_6)$. The stability proof is similar to the proof of Theorem 1 in [13] and is omitted here for brevity.

B. FTSM Controller

Consider that $M, C(\ )$ and $g(\ )$ are known, then the following control law for the equation (6) is proposed

$$= C(\ )\ + g(\ ) + MJ\ ^1[\ \dot{J}(\ )\ + \dot{}_d + \ _2]; \tag{18}$$

where $_d$ is the desired position vector seen in the inertial system, substituting (18) in (6) we obtain

$$\dot{} \quad \dot{}_d = \ _2 + \ _2; \tag{19}$$

where $_2 = J(\ )M\ ^1[\quad D(\ )\ ]$. Define $e = \quad _d$ and based in [17] the following sliding surface $s\ 2\ \mathbb{R}^6$ is proposed

$$s = \dot{e} + Ae + Be^{M_n} \tag{20}$$

$$\dot{s} = \quad As \quad B\text{sign}(s); \tag{21}$$

where $\text{sign}(s) = [\text{sign}(s_1); :::; \text{sign}(s_6)]^T$ and $e^{M_n} = [e_1^{M_1}; :::; e_6^{M_6}]^T$.

Theorem 2

For the dynamic model of an AUV (6), if the sliding surface is chosen as (20), the reaching law is chosen as (21) and the continuous is designed as

$$_2 = \quad A(\dot{e} + s) \quad M_n B\dot{e}^{M_n} \quad B\text{sign}(s); \tag{22}$$

Then the system trajectory will converge to the neighborhood of sliding surface $s = 0$. The stability proof is similar to the proof of Theorem 1 in [17] and is omitted here for brevity.

V. NUMERICAL SIMULATIONS

In this section, the numerical results of the control algorithm for trajectory tracking are presented, where two different trajectories are proposed. The trajectory tracking is realized autonomously applying the control laws proposed in the equations (12) and (17). The underwater vehicle has a mass of $17{:}94kg$ and dimensions of $70 \quad 40 \quad 47cm$. Table (I) describes the physical, dynamic parameters of the vehicle, meanwhile the Euler's angle control gains with quaternions are expressed in the Table (II) and dynamic parameters of the vehicle, meanwhile the Euler's angle control gains are expressed in the Table (III). The control gains are chosen such that (16) is fulfill.

Param.	Value.	Param.	Value.	Param.	Value.
W	$[0; 0; 176]^T$	$X_{\dot{u}}$	5.5	$Y_{\dot{v}}$	12.7
$\ _b$	$[0; 0; \quad 0{:}1]^T$	$Z_{\dot{w}}$	14.57	I_{xx}	0.16
B	$[0; 0; 9{:}81m_f]^T$	I_{yy}	0.16	I_{zz}	0.16
$K_{\dot{p}}$	0.002	$M_{\dot{q}}$	0.002	$N_{\dot{r}}$	0.12
X_u	3.03	Y_v	3.21	Z_w	8.18
K_p	2	M_q	0.1	N_r	0.07
X_{u_c}	4.03	Y_{v_c}	6.21	Z_{w_c}	5.18
K_{p_c}	0.07	M_{q_c}	0.07	N_{r_c}	0.07

TABLE I
PHYSICAL AND DYNAMIC PARAMETERS OF THE VEHICLE.

Param.	Value.	Param.	Value.	Param.	Value.
A_1	3	A_2	3	A_3	2
A_4	19	A_5	1	A_6	1
B_1	2	B_2	1	B_3	0.8
B_4	0.01	B_5	1	B_6	1
$_1$	1.9	$_2$	1.5	$_3$	2.3
$_4$	2.1	$_5$	1.2	$_6$	1.2
$_1$	1.8	$_2$	1.5	$_3$	1.09
$_4$	1.8	$_5$	1.1	$_6$	1.1
M_1	0.5	M_2	2	M_3	1.3
M_4	1	M_5	1	M_6	1
$k_{1:1}$	1.15	$k_{1:2}$	0.215	$k_{1:3}$	0.4
$k_{1:4}$	10	$k_{1:5}$	1	$k_{1:6}$	0.8
$k_{2:1}$	1.15	$k_{2:2}$	0.215	$k_{2:3}$	0.31
$k_{2:4}$	10	$k_{2:5}$	1	$k_{2:6}$	0.8

TABLE II
CONTROL GAINS FOR THE MODEL WITH QUATERNIONS.

Param.	Value.	Param.	Value.	Param.	Value.
A_1	2.4	A_2	2.2	A_3	2
A_4	0.1	A_5	3	A_6	0.9
B_1	0.09	B_2	0.006	B_3	0.001
B_4	0.002	B_5	0.0035	B_6	0.055
M_1	3	M_2	2	M_3	2
M_4	2	M_5	2	M_6	2

TABLE III
CONTROL GAINS FOR THE MODEL WITH EULER'S ANGLES.

A. Quaternion simulation.

In the first test, the vehicle starts from the initial conditions $P_0 = [0{:}0; 0{:}09]^T$ and $q_0 = 1$, with a trajectory q_{tr} proposed in the equation (23), which represents the contour of a sphere,

$$\begin{aligned} P_{I_d} &= q_{tr} \quad \ \quad q_{tr}^* + \ + 0{:}09k \\ q_{tr} &= \cos\ \frac{}{2}\ \cos\ \frac{^2}{2} \quad i\sin\ \frac{}{2}\ \sin\ \frac{^2}{2}\ + \\ & \quad j\cos\ \frac{}{2}\ \sin\ \frac{^2}{2}\ + k\sin\ \frac{}{2}\ \cos\ \frac{^2}{2} \\ q_d &= \cos(\ \ =2) + k\sin(\ \ =2); \end{aligned} \tag{23}$$

where $r = [0; 0; 5]^T$, $_2 = [1 + t/180]$ and $= 4\ t/63$. For this case, the vehicle modifies its orientation so that it keeps facing at all times towards the center of the trajectory.

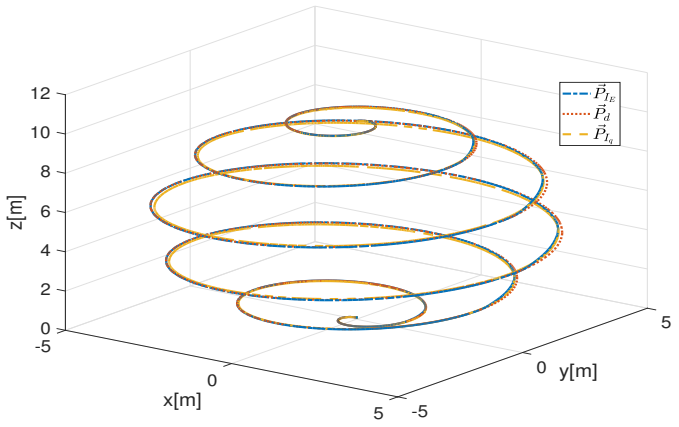

Fig. 3. Autonomous trajectory tracking. P_{I_E} is the inertial system trajectory with Euler's angle control, P_{I_E} is the desired trajectory and P_{I_q} is the inertial system trajectory with quaternion control .

In Figure 3 and 4, it can be seen that the position of the vehicle during the tracking of the trajectory achieves the desired behavior. We can appreciate that the proposed strategy is good enough to carry out this task. Figure 5 shows the evolution of the quaternion and we can notice that the desired orientation is achieved.

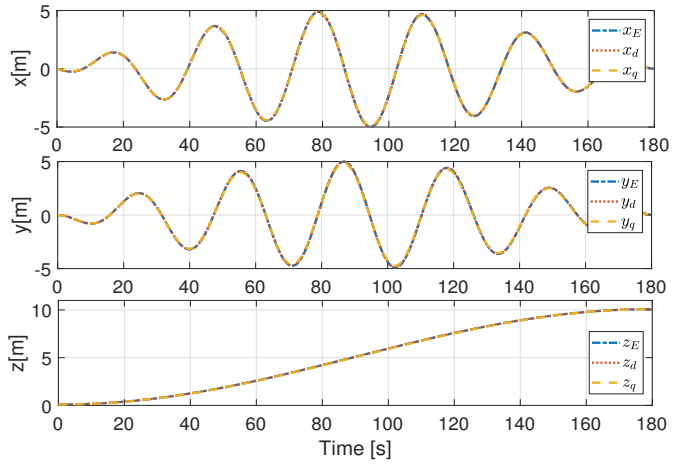

Fig. 4. The actual and desired position of the AUV in x y z axes using the proposed trajectory tracking controllers. Where x_E y_E z_E are the inertial system trajectory with Euler's angle control, x_d y_d z_d are the desired trajectory and x_q y_q z_q are the inertial system trajectory with quaternion control.

The control signals are presented in Figure 6. Notice that the control inputs generated by the NFTSMC has a significant chattering reduction.

B. Euler's angle simulation.

In the simulation with Euler angles that is represented in equation (6), the same trajectory of equation (23) was used, with

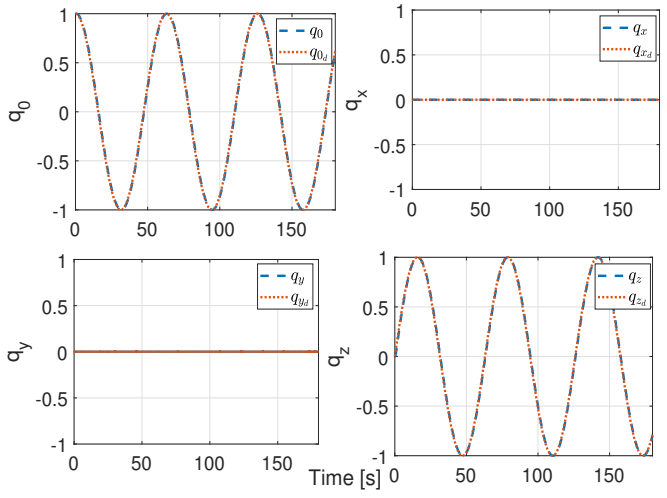

Fig. 5. Tracking simulation results for the actual and desired quaternion of the underwater vehicle in the sphere-trajectory.

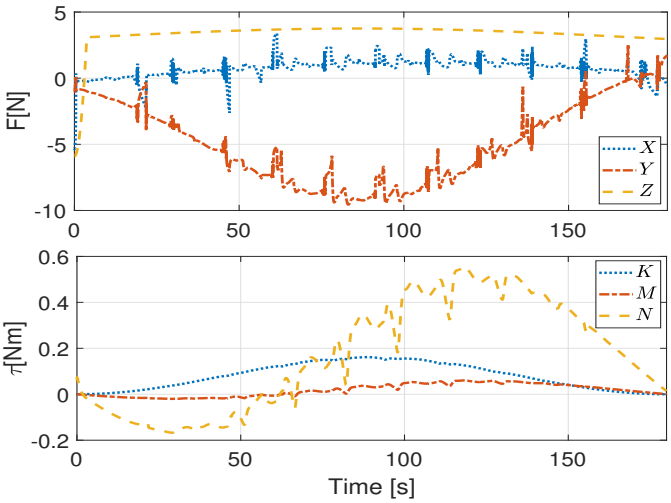

Fig. 6. Control inputs based on NFTSMC for the Fossen model with quaternions, a significant attenuation of the chattering effect is noted .

the same initial conditions, i.e. $_0 = [0; 0; 0.09; 0; 0; 0]^T$ and $_0 = [0; 0; 0; 0; 0; 0]^T$. For the comparison of the monitoring of the angular trajectory of the two controllers, the quaternions of the Figure 4 were transformed to Euler angles, which is shown in the Figure 7. Note that in the Figure 7 it can be observed that the trajectory tracking was performed better with quaternions than with Euler angles, this is due to the singularity of the Euler angles at points 180 and 180 since when it reaches 180 and you want to get 180 first make almost a turn in the opposite direction, situation that does not happen with quaternions.

In Figure 3 and 4, it can be seen that with both controllers, the trajectory tracking is efficient, but when comparing Figures 6 and 8 it is observed that the FTSM control has more chattering than with NFTSMC.